land

MDPI

Article

Evaluating Modified Soil Erodibility Factors with the Aid of Pedotransfer Functions and Dynamic Remote-Sensing Data for Soil Health Management

Pooja Preetha [1,*] and Naveen Joseph [2]

[1] Department of Mechanical & Civil Engineering and Construction Management, College of Engineering, Technology, and Physical Sciences, Alabama A&M University, Huntsville, AL 35811, USA
[2] Department of Geospatial Science, Artis College of Science and Technology, Radford University, Radford, VA 24142, USA; njoseph2@radford.edu
* Correspondence: pooja.preetha@aamu.edu

Abstract: Soil erosion is a critical factor impacting soil health and agricultural productivity, with soil erodibility often quantified using the K-factor in erosion models such as the universal soil loss equation (USLE). Traditional K-factor estimation lacks spatiotemporal precision, particularly under varying soil moisture and land cover conditions. This study introduces modified K-factor pedotransfer functions (Kmlr) integrating dynamic remotely sensed data on land use land cover to enhance K-factor accuracy for diverse soil health management applications. The Kmlr functions from multiple approaches, including dynamic crop and cover management factor (Cdynamic), high resolution satellite data, and downscaled remotely sensed data, were evaluated across spatial and temporal scales within the Fish River watershed in Alabama, a coastal watershed with significant soil–water interactions. The results highlighted that the Kmlr model provided more accurate sediment yield (SY) predictions, particularly in agricultural areas, where traditional models overestimated erosion by upto 59.23 ton/ha. SY analysis across the 36 hydrological response units (HRUs) in the watershed showed that the Kmlr model captured more accurate soil loss estimates, especially in regions with varying land use. The modified K-factor model (Kmlr-c) using Cdynamic and high-resolution soil surface moisture data outperformed the traditional USLE K-factors in predicting SY, with a strong correlation to observed SY data (R^2 = 0.980 versus R^2 = 0.911). The total sediment yield predicted by Kmlr-c (525.11 ton/ha) was notably lower than that of USLE-based estimates (828.62 ton/ha), highlighting the overestimation in conventional models. The identification of erosive hotspots revealed that 6003 ha of land was at high erosion risk (K-factor > 0.25), with an average soil loss of 24.2 ton/ha. The categorization of erosive hotspots highlighted critical areas at high risk for erosion, underscoring the need for targeted soil conservation practices. This research underscores the improvement of remotely sensed data-based models and perfects them for the application of soil erodibility assessments thus promoting the development of such models.

Keywords: K-factor; C-factor; remote sensing; soil surface moisture; land cover

check for updates

Academic Editor: Claude Hammecker

Received: 24 February 2025
Revised: 15 March 2025
Accepted: 18 March 2025
Published: 20 March 2025

Citation: Preetha, P.; Joseph, N. Evaluating Modified Soil Erodibility Factors with the Aid of Pedotransfer Functions and Dynamic Remote-Sensing Data for Soil Health Management. *Land* **2025**, *14*, 657. https://doi.org/10.3390/land14030657

Copyright: © 2025 by the authors. Licensee MDPI, Basel, Switzerland. This article is an open access article distributed under the terms and conditions of the Creative Commons Attribution (CC BY) license (https://creativecommons.org/licenses/by/4.0/).

1. Introduction

Soil erosion has long been a focus of research and land management because of its significant effects on agriculture [1,2], water quality [3,4], and ecosystem services [5]. The universal soil loss equation (USLE) is widely used to estimate soil erosion rates based

on factors such as rainfall erosivity (R), soil erodibility (K), slope length and steepness (LS), crop cover and management (C), and conservation practices (P) [6]. Among these, the K-factor, which represents soil susceptibility to erosion, is crucial for determining erosion potential in an area and is typically calculated using empirical relationships based on soil texture, organic matter content, and other physical characteristics [7]. However, traditional K-factor estimates, which rely on soil survey data or laboratory analyses, often lack the spatial and temporal resolution required for accurate, real-time assessments of soil erodibility, failing to capture variations due to factors such as moisture content and land cover changes, which are vital for predicting erosion processes [8].

Despite the widespread use of the USLE, its application is limited by the static nature of the K-factor estimation [9]. For example, soil moisture significantly affects erodibility, with wet soils being more resistant and dry soils more prone to erosion [10]. However, traditional K-factor models often fail to account for these dynamic variations in soil moisture, which are influenced by rainfall patterns, irrigation, and seasonal changes [11]. Additionally, land cover and vegetation help reduce erosion by protecting soil from raindrop impact and slowing runoff [12], yet the K-factor does not consider land cover changes. This highlights the need for a more adaptable method to estimate the K-factor, one that accounts for dynamic environmental factors for improved soil health management.

Sediment yield prediction is another critical component for understanding soil erosion, water quality management, and agricultural sustainability [13,14]. However, the traditional approaches, using the USLE and its variation like the Revised USLE (RUSLE) [15], focus mainly on soil erosion, not the actual sediment yield reaching downstream locations. Hence, there is a need for models that consider sediment transport processes and sediment delivery ratios (SDR), which account for the proportion of eroded material reaching rivers or reservoirs. To account for this problem, recent studies have adopted physically based models such as WEPP (Water Erosion Prediction Project) and SWAT (Soil and Water Assessment Tool), which can simulate interactions between precipitation, runoff, soil erosion, and sediment transport [16–20]. Additionally, machine learning and AI approaches, such as neural networks and support vector machines (SVMs), have emerged as effective tools for sediment yield prediction [21–23]. These models analyze large datasets, including climate, land use, and soil properties, to predict sediment yield based on observed patterns. Furthermore, high-resolution data from remotely sensed imagery or geographic information system (GIS) improves spatiotemporal predictions, enhancing sediment transport management across watersheds [24,25].

The relationship between the K-factor and sediment yield is complex, as the K-factor measures soil susceptibility to detachment, while sediment yield also depends on the transport, deposition, and delivery of eroded material [26]. Recent studies have integrated the K-factor with dynamic variables such as soil moisture, land cover, and precipitation to refine sediment yield predictions [27,28]. In these models, the K-factor serves as a baseline for predicting potential erosion, while other factors (e.g., vegetation, slope, and land management) help refine the sediment transport process to accurately estimate sediment yield. For instance, dynamic K-factors that vary with changing soil moisture and land cover have been shown to improve sediment yield predictions by adjusting the soil erodibility estimates in real-time, making the model more sensitive to seasonal or climatic variations [29]. Moreover, integrating the K-factor with hydrological models such as SWAT, sediment yield estimates can be made not only based on the erodibility of the soil but by incorporating watershed-scale factors, such as flow direction, runoff, and sediment deposition patterns [30].

Recent advancements in remote sensing technologies, including high-resolution satellite data from the Moderate Resolution Imaging Spectroradiometer (MODIS), Landsat, and

Sentinel, have improved soil erosion models by providing real-time, spatially distributed information on environmental factors such as land cover, vegetation, and soil moisture [31]. These technologies offer advantages over traditional soil sampling by capturing variables with high temporal frequency and at a global scale [32]. Moreover, studies have demonstrated that integrating remote sensing data, such as vegetation indices and soil moisture content, into erosion models enhances soil erodibility predictions [33,34]. This approach offers a dynamic, real-time method for assessing soil erodibility, particularly in regions with rapidly changing conditions.

A combination of remote sensing, hydrological modeling, and pedotransfer functions are increasingly being utilized to improve sediment yield estimates by incorporating dynamic, real-time data and integrating spatial and temporal variations that traditional methods might overlook. Pedotransfer functions are mathematical models that estimate soil properties from easily measurable attributes like texture and bulk density and are widely used in soil science to predict properties such as hydraulic characteristics and organic matter content [35–37]. Remote sensing technologies, particularly from satellite and airborne sensors, provide high-resolution data on various environmental parameters such as land cover, vegetation indices, soil moisture, and topography [38]. Satellite imagery, such as that from the Sentinel-2 or Landsat series, allows for frequent, large-scale monitoring of soil and land cover characteristics, which are critical for predicting sediment yield [39]. Vegetation indices derived from remote sensing (e.g., NDVI—normalized difference vegetation index) are particularly useful in assessing land cover, which can mitigate soil erosion by protecting the soil surface from rainfall and runoff [40]. Additionally, soil moisture content, which can be obtained from remote sensing platforms such as SMOS (Soil Moisture and Ocean Salinity), is a key factor influencing soil erodibility [41]. Wet soils are generally less erodible than dry soils, and remote sensing data can help model soil moisture dynamics more accurately, providing a better foundation for sediment yield predictions. Furthermore, advanced techniques, such as geospatial modeling, allow for the integration of high-resolution spatial data into watershed-scale models, enabling more accurate predictions of sediment yield at different scales [42]. Thus, by integrating pedotransfer functions with remote sensing data, the K-factor can be adjusted based on changing environmental conditions, such as moisture content and vegetation cover, which in turn improves the accuracy of sediment yield predictions. Moreover, pedotransfer functions can be used in combination with machine learning algorithms, which can analyze large datasets from remote sensing and ground measurements to estimate sediment yield with high accuracy [43]. These hybrid models offer the advantage of capturing complex, nonlinear relationships among soil properties, land cover, and sediment transport, which traditional methods might miss. By incorporating real-time data into the modified K-factor, this research offers a more accurate, responsive model for assessing soil erodibility, which can greatly enhance erosion risk prediction, improve soil health management, and contribute to more sustainable agricultural practices globally.

The main purpose of this study is to improve the accuracy of soil erodibility factor estimates by implementing a modified K-factor pedotransfer function that integrates dynamic, remotely sensed data, such as land use land cover and soil moisture. The novel model aims to provide more accurate and spatiotemporally precise predictions of soil erosion and sediment yield, particularly by incorporating factors such as soil moisture variations, crop and cover management, and high-resolution satellite data. The significance of this study lies in its ability to enhance soil health assessments and agricultural productivity by offering a more tailored and accurate model for predicting soil erosion, especially in regions with complex soil–water interactions. The findings underscore the importance of using dynamic data for better watershed management and soil conservation strategies, ultimately improving soil health, ecosystem resilience, and land management practices.

2. Materials and Methods

2.1. Datasets for the Study Area

In this study, the watershed modeling was performed using a process-based hydrological model, the Soil and Water Assessment Tool (SWAT). The SWAT model was employed to delineate the study area of the Fish River watershed, with an area of 783 sq.km. The model inputs included digital elevation models (DEM), land use land cover data, soil data, and meteorological data (Table 1). The model classified the delineated watershed into 7 subbasins and 36 hydrological response units (HRU). Each HRU is a specific combination of a particular land use land cover, a particular soil type, and a particular slope gradient. Then, the meteorological data were fed into the model, and the model was calibrated and validated for the spatial units of subbasins and HRUs and temporal scales of years and months. All the simulations from the SWAT model produced outputs in three different spatial scales, the watershed level, subbasin level, and HRU level. The study also employed MODIS-based yearly data on land use land cover and undertook supervised classification of the land use land cover data to capture the temporal land cover changes, which have implications on soil erosion rates and soil health in the watershed. The land cover dynamics were reflected through the crop and cover management factor (C-factor) used in the study. Figure 1 shows the Fish River watershed with land cover dynamics spatially spread across the watershed. The SWAT model outputs predicted the sediment yield (SY) for the watershed, subbasins, HRUs, and reaches for Fish River watershed between 2001 and 2011.

Table 1. Materials and datasets employed for the watershed modeling of the study area.

Dataset	Sources	Data Type	Spatial Resolution	Temporal Resolution	Details
Digital Elevation Models	Web GIS	Raster	30 m	Yearly, 2001–2011	Supplies elevation data for analyzing terrain and delineating watersheds
Land Cover	United States Geological Survey (USGS)	Raster	30 m	Yearly, 2001–2011	Comprises 8 land use types, which are utilized to model the impacts of land cover on hydrology
Soil	United States Department of Agriculture (USDA)	Raster	60 m	Yearly, 2001–2011	Contains data on 5 soil types with hydrological properties, crucial for understanding soil–water interactions
Meteorology	U.S. National Weather Service	Gridded Data	1 km	Yearly, 2001–2011	Provides data on temperature, precipitation, wind speed, solar radiation, and relative humidity, which were used in Arc SWAT's weather generator
Hydrology	United States Geological Survey (USGS)	Gridded Data	1 km	Monthly, 2001–2011	Offers surface runoff and sediment concentration data from hydrological stations (Silver Hill and Loxley River)
Crop Management Factor	Remote Sensed MODIS Data	Raster	250 m	Yearly, 2001–2011	Supplies crop management data that reflect land use and agricultural practices influencing hydrological processes

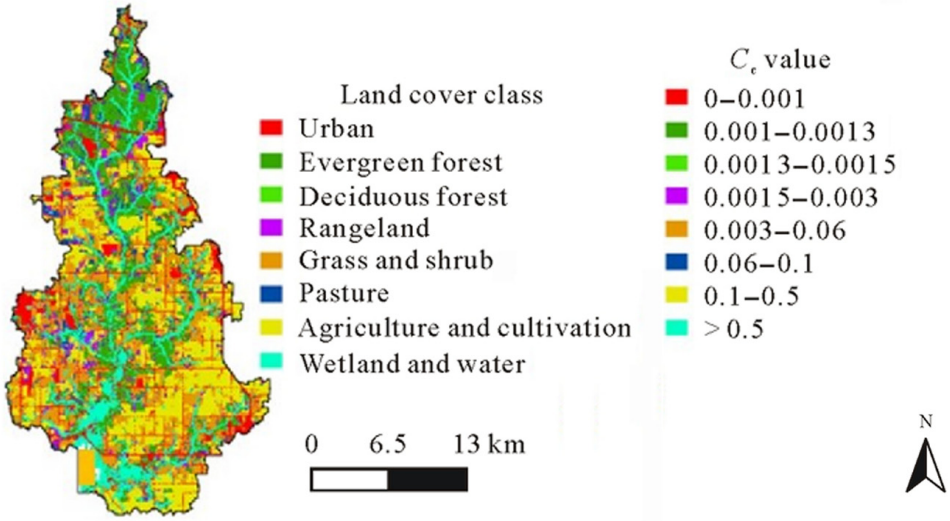


Figure 1. Map showing the annual land cover classifications and the corresponding C-factors (Ccs) values for Fish River watershed.

2.2. Kmlr Modeling

The K_{USLE} for each type of soil with corresponding land cover was obtained from the SWAT model using the following equation [44]:

$$K_{USLE} = \left[0.00021 \times M^{1.14} \times (12 - OM) + 3.25 \times (c_{soilstr} - 2) + 2.5 \times (c_{perm} - 3)\right]/100 \quad (1)$$

where M is the particle size parameter, OM is the organic matter content of the soil (%), $c_{soilstr}$ is the soil structure code used in soil classification, and c_{perm} is the profile permeability class. The K_{USLE} is referred to as the soil loss rate for every unit of soil erosivity in a specific soil as surveyed or observed on a unit plot [45].

The overestimation of the soil loss estimates by the USLE, RUSLE, and extensions of USLE such as MUSLE, USLE-M, and dUSLE have resulted in novel approaches to dynamically and realistically assess K-factors, especially in catchments [46–48]. This study introduces a modified K-factor pedotransfer function uisng multiple linear regression modeling (Kmlr) integrating dynamic, remotely sensed data on soil surface moisture and land cover to enhance K-factor accuracy for diverse soil health management applications. The dynamic functionality of the K-factor in the study was developed using the topographic factor (LS_{USLE}), the C-factor, and the soil properties of soil surface moisture (AWC in %), bulk density (BD in g/cm^3), and permeability (P_{soil} in mm/h). While the original USLE is designed for bare soil, many applications of erosion modeling in more practical, real-world scenarios require accounting for vegetation to more accurately predict erosion rates in catchments or landscapes that are not bare fallow. The study area contains an assortment of land use land covers, as indicated below, which justified the need to use a crop management factor in the Kmlr equation to find the soil erodibility factor (Figure 1).

The topographic factor, LS_{USLE}, and C-factor were calculated using the equation in [49]. The values of the variables, such as AWC, BD, and P_{soil}, were obtained from the model outputs of watershed delineation identified for the corresponding HRUs. The slope, S, was calculated from DEMs of the watershed. After categorizing the watershed into HRUs, the HRU map, along with S and DEM, and the flow direction map were used to calculate HRU-wise estimates of slope and longest flow length. The calculated longest flow length in each HRU was taken as the slope length, L for the corresponding HRUs in the watersheds. The following operations were executed in the GeoHMS terrain processing tool as well as the raster calculator in GIS. Thus, the variables of L and S used in the calculation of topographic factors were obtained from the watershed delineation results spatially joined

to the corresponding HRUs from 2001 to 2011 in the watershed. The soil properties of BD and P_{soil} were obtained from the soil attribute characterization module (.sol) of the SWAT model. They were calculated by the spatial join of the soil map (soil type) and HRU map (HRU ID) in the SWAT model. Thus, the developed model of K-factor, Kmlr, serves as a dynamic and realistic improvement of the K_{USLE} equation in terms of capturing the HRU-wise and annual variations in soil erodibility and is given here [50]:

$$\text{Kmlr} = -0.064 + 0.173\text{AWC} + 0.122\text{BD} - 0.000044\text{P}_{soil} + 7.699\text{LS}_{USLE} + 0.0081\text{C} - \text{factor} \quad (2)$$

Both K_{USLE} and Kmlr are expressed as ton acre hour per acre feet ton inch in U.S. customary units (metric ton. hectare.hour per hectare.megajoule.millimeter in S.I. units). The coefficients presented in Equation (2) were employed, and the developed K-factor model was calibrated with the historical soil erodibility factor estimates, yielding substantial performance improvements in the study areas (R^2 = 0.903, PR^2 = 0.821, $p < 0.05$ [50]). The workflow describing the SWAT model development and simulations using SWAT-based inbuilt K-factors, along with the later phase where K-factor modification was performed using the additional soil properties of soil surface moisture and soil bulk density, is shown in Figure 2.

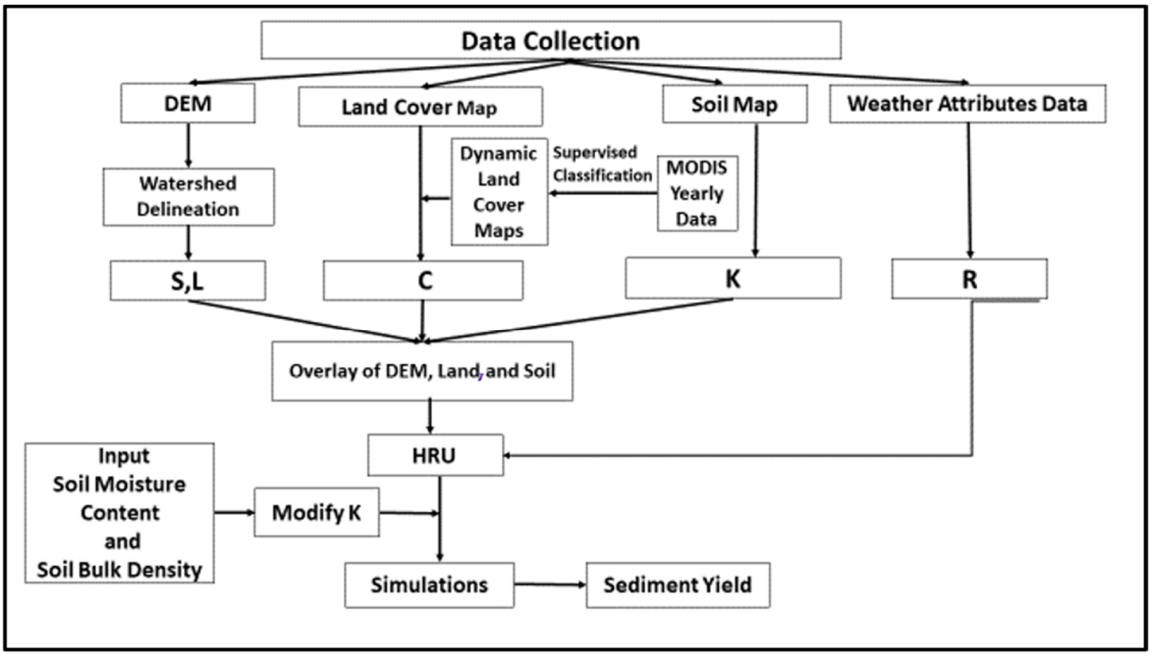


Figure 2. Methodology applied for the generation of a modified K-factor for annual estimates of soil erodibility and soil loss in watersheds, subbasins, and HRUs.

2.3. Kmlr Modification Approaches

2.3.1. High-Resolution Satellite Data in Kmlr

High-resolution satellite data enhance the spatial and temporal accuracy of soil property estimation, providing essential information on land cover, vegetation indices, soil moisture, and topographic features that are crucial for calculating the K-factor. The soil surface moisture estimates, which are vital for calculating the K-factor, could be generated from satellite data with higher resolution, providing detailed information on soil moisture profiling at a fine resolution. The steps used in this modification process were as follows:

1. Replace STATSGO soil data with satellite-derived soil moisture data.
2. Process the satellite-derived soil moisture data for integrating into GIS with spatial compatibility.

3. Integrate the satellite-derived soil moisture data into ArcGIS (which operates on GIS principles) and superimpose it for the study area boundary.
4. Analyze the integrated data and generate spatially changing soil moisture data, AWC, for the study area.
5. Incorporate AWC data into the SWAT model to estimate the K-factors and SY.

2.3.2. Dynamic C-Factors in Kmlr

In the context of the Kmlr model, high-resolution satellite imagery enables the accurate estimation of the crop and cover management factor, which varies annually depending on land cover and vegetation dynamics. In the Kmlr model, the USLE K-factor is modified by incorporating dynamic factors inbuilt in the hydrological model such as soil surface moisture, bulk density, and permeability, which change seasonally or annually across a watershed. Hence, the Kmlr model was modified with the aid of dynamic C-factors representing real land cover changes and satellite-derived, spatially changing soil moisture data. The steps used in this modification process were as follows:

1. Acquire high-resolution satellite imagery of enhanced vegetation index (EVI), fraction of photosynthetically active radiation (SR), and leaf area index (LAI) to develop the dynamic C-factor, Cdynamic, functionality for the study area.
2. Process EVI, SR, and LAI data for integration into GIS with spatial compatibility.
3. Integrate EVI, SR, LAI, and the developed AWC data into ArcGIS and superimpose it for the study area boundary.
4. Calculate Cdynamic for the HRUs and subbasins of the study area.
5. Modify the Kmlr model by incorporating the Cdynamic estimates.
6. Incorporate the modified Kmlr model estimates into the SWAT model to estimate the SY.

2.3.3. Downscaled Satellite Data in Kmlr

The use of downscaled data and data products is crucial for adapting coarse global or regional climate and land-use models to local conditions, especially in heterogeneous landscapes with varied soil types and land management practices [51,52]. By integrating these downscaled datasets with SWAT model outputs, the Kmlr model can more accurately capture the temporal and spatial variations in soil properties, land cover, and topography. This leads to a more realistic and adaptive K-factor calculation that can respond to environmental changes, such as changing precipitation patterns or vegetation cover, thus improving the reliability of sediment yield predictions. The steps used in this modification process are as follows:

1. Obtain downscaled satellite imagery of soil moisture from Soil Moisture Active Passive (SMAP).
2. Refine spatial scales of SMAP data using the tool GeoDa and resampling methods.
3. Integrate the refined SMAP data into ArcGIS and superimpose it for the study area boundary.
4. Incorporate SMAP data generated in Step 3 and Cdynamic estimates together to modify the Kmlr model.
5. Incorporate the modified Kmlr model estimates into the SWAT model to estimate the SY.

2.4. Sediment Yield Predictions

Sediment yield predictions are crucial for understanding soil erosion dynamics, assessing water quality, and managing soil health. Accurate predictions help in developing effective soil conservation strategies and managing the impacts of erosion on agricultural

productivity. The study used SWAT (Soil and Water Assessment Tool) for predicting the sediment yield responses in the watershed, subbasins, and HRUs from 2001 to 2011. The sediment yield was simulated in the SWAT model for the three spatial units of the basin, the watershed, subbasins, and HRUs, under the five developed Kmlr scenarios listed in Sections 2.2 and 2.3. The sediment yield in ton/ha was calculated based on K_{USLE}, Kmlr, Kmlr-c, Kmlr-sat, and Kmlr-dsat and validated against the ground truth estimates.

2.5. Erosive Hotspots

Identifying hotspots of erosion based on K-factor categorization or sediment yield prediction within a watershed is essential for targeted erosion control and land management strategies. These hotspots represent areas where erosion and sediment transport are particularly intense because of factors such as steep slopes, vulnerable soil types, or insufficient vegetation cover. By analyzing such hotspots across different spatial units, such as HRUs or subbasins in a watershed, it is possible to identify areas most at risk of erosion and prioritize interventions. By coupling these erosion-based hotspot data with the spatial sediment yield predictions from SWAT, it is possible to generate spatial maps of significant sediment yield across the watershed. These maps can be used by land managers to identify and address areas where erosion control measures, such as vegetation restoration or sediment retention structures, would be most effective.

3. Results

3.1. Kmlr Model Modification Results

3.1.1. Kmlr-Sat Modeling Using High-Resolution Satellite Data

The traditionally used STATSGO soil data generated AWC modeled estimates with a spatial resolution of 1 km × 1 km and provided a constant soil moisture variable of AWC for the entire simulation period [53]. This task replaced the STATSGO dataset with spatially changing soil moisture data derived from the remotely sensed satellite imagery of AWC based on the surface reflectance dataset of MODIS with a spatial resolution of 250 m × 250 m. The task aimed to investigate the enhancement in the spatial representation of K-factor outcomes with finer spatially resolute satellite-derived data. The analysis was conducted using Python programming 3.13.2, ArcGIS, and the Google Earth Engine Code Editor. The remotely sensed environmental data on AWC were obtained for each pixel of the derived images for the watershed. These datasets were extracted for the Fish River watershed from the LP DAAC database for the period 2001–2011. AWC refers to the soil moisture percentage in the surface soil layer and had a resolution of 250 m. The model developed is referred to as Kmlr-sat (Kmlr + MODIS based AWC data).

$$\text{Kmlr} - \text{sat} = -0.064 + 0.173\text{AWC(MODIS)} + 0.122\text{BD} - 0.000044\text{P}_{\text{soil}} + 7.699\text{LS}_{\text{USLE}} + 0.0081\text{C} - \text{factor} \quad (3)$$

3.1.2. Kmlr-c Modeling Using Dynamic C-Factors

To refine the K-factor, the modified K-factor model, Kmlr-c, introduces an additional dynamic factor, Cdynamic (Kmlr + MODIS based AWC data + MODIS based Cdynamic equation).

$$\text{Cdynamic} = 0.203 - 0.007\exp\left(\frac{-\text{aEVI}}{\text{b} - \text{EVI}}\right) - 0.094\text{SR} + 0.006\text{LAI} + 0.0001\text{AWC} + 0.0001\text{A} - 0.003\text{S} \quad (4)$$

where Cdynamic is the crop and cover management factor [54]. The developed C-factor model implements the satellite remotely sensed data on enhanced vegetation index (EVI), fraction of photosynthetically active radiation (SR), leaf area index (LAI), ratio of the area of hydrologic response unit to the total watershed area (A), and slope gradient (S). a and b are

parameters that determine the shape of the exponential curve of C and EVI. Values of 1.5 and 1 was assigned for a and b, respectively and the coefficients presented in Equation (3) were employed, which yielded the best fit for the C-factor model, Cdynamic, for the study areas (R^2 = 0.68, PR^2 = 0.51, $p < 0.05$) [54]. The modified Kmlr equation is as follows:

$$\text{Kmlr} - \text{c} = -0.064 + 0.173\text{AWC(MODIS)} + 0.122\text{BD} - 0.000044\text{P}_{\text{soil}} + 7.699\text{LS}_{\text{USLE}} + 0.0081\text{Cdynamic(MODIS)} \quad (5)$$

In this study, we utilized the remotely sensed satellite imagery of EVI, LAI, SR, and AWC from MODIS. The task aimed to investigate the enhancement in the spatial representation of K-factor outcomes with a collection of four sets of finer, spatially resolute satellite-derived data. The EVI, AWC, LAI, and SR values were obtained for each pixel of the derived images for the watershed from the LP DAAC database for the period 2001–2011. The EVI data (product ID: MOD13Q1) had a spatial resolution of 250 m, while the LAI and SR data product (MOD15A2H) had a resolution of 500 m. LAI is defined as the ratio of half the total surface area of leaves to the unit ground area, while SR represents the fraction of photosynthetically active radiation absorbed by green vegetation, as identified in the MODIS data product subset.

3.1.3. Kmlr-dsat Modeling Using Downscaled Satellite Data

In this study, the downscaled soil moisture data obtained from the satellite product Soil Moisture Active Passive (SMAP) were refined to finer spatial scales using the spatial data analysis software GeoDa 1.22. Data from the SMAP Enhanced L3 Radiometer Global Daily 9 km EASE-Grid Soil Moisture Version 3 (SPL3SMP_E) product, spanning from 2001 to 2011, were utilized in this task [55]. The study used the inverse distance weighted method and nearest neighbor resampling method to improve the raw SMAP data's spatial resolution of 9 km to 1 km [56,57]. GeoDa's strength lies in spatial analysis, and it can be useful for understanding spatial patterns after resampling. The model developed is referred to as Kmlr-dsat (Kmlr + SMAP based downscaled AWC data + SMAP and MODIS based Cdynamic equation).

$$Kmlr - dsat = -0.064 + 0.173AWC\ (SMAP) + 0.122BD - 0.000044P_{soil} + 7.699LS_{USLE} + 0.0081Cdynamic\ (MODIS + SMAP) \quad (6)$$

3.2. Results of Descriptive Statistics of Kmlr Model

Table 2 explains the descriptive statistics of the modeled soil properties, topographical factors, and land cover attributes for Kmlr estimation. The data indicate that while the soil textural property of AWC remained relatively stable in some parts of the watershed over a ten-year period, most of the HRUs showed yearly variations in AWC, reflecting changes in water availability or seasonal influences. Soil permeability varied greatly, with a significant range from 27.67 mm/h to 650 mm/h, reflecting the diversity of soil types and drainage characteristics within the watershed. The high maximum value suggests the presence of highly permeable soils in some regions. Bulk density and soil permeability also exhibited annual variations, which could be attributed to local soil management practices, land use changes, or climatic fluctuations. The LS_{USLE} factor, related to the topography of the land and its influence on erosion, showed a broad range, with some areas highly susceptible to erosion (higher values) and others relatively stable. The C-factor represents the effect of land cover and land management practices on soil erosion. Its range suggests a diversity of land cover types, with some areas having little to no impact on erosion (C-factor nearing 0) and others contributing significantly (C-factor close to 1), reflecting land cover's role in reducing or enhancing soil erosion. These variations highlight the dynamic nature of these

soil and landscape properties and suggest the need for periodic monitoring and assessment to understand their role in watershed management and erosion control [58].

Table 2. Descriptive statistics of the physicochemical properties of the studied soils, topographical factors, and land cover attributes for Kmlr estimation.

Descriptive Statistics	AWC (%)	Psoil (mm/h)	BD (g/cm^3)	LSUSLE	C-Factor
Mean	0.33	58.18	1.04	3.12	0.386
Minimum	0.11	27.67	0.98	0.65	0
Maximum	0.69	650	1.53	15.11	1

3.3. Results of Descriptive Statistics of Modified Kmlr Models

The Cdynamic data used in the Kmlr-c model were integrated from both SWAT model outputs and satellite data, providing real-time, high-resolution spatial data that accounted for seasonal and annual changes in soil properties. This model captures the variations in soil erodibility due to soil surface moisture, land cover, and topography, thus improving the accuracy of sediment yield predictions compared with traditional K-factor models. Besides this, the values of Cdynamic using Equation (3) were used as the explanatory variables of the C-factor in Equation (2) annually for every HRU. This indicated that there was a dynamic improvement in K-factor prediction using Kmlr-c, which was a function of the dynamic crop and cover management factor. Table 3 explains the descriptive statistics of the remotely sensed and modeled soil properties for K-factor estimation using Cdynamic. The dataset suggests a diverse landscape in the study area, with varying soil moisture, permeability, density, vegetation cover, and slope characteristics. The minimum AWC value of 0.13% indicates areas with very low water retention capacity, possibly due to coarse or sandy soils, while the maximum value of 0.73% suggests regions with high water retention potential likely due to clayey or organic-rich soils. The significant variability in these factors implies that different areas within the watershed may have distinct hydrological and erosion dynamics. The mean EVI value of 0.33 indicates moderate vegetation cover in the area. The minimum value of 0.11 suggests sparse or no vegetation in some areas, such as bare soil or urban zones, while the maximum value of 0.6 indicates areas with healthy vegetation or dense grasslands. This variability impacts the accurate estimation of the K-factor and understanding soil erosion and runoff processes within the watershed, with the dynamic changes in vegetation and soil properties influencing the watershed's overall environmental response.

Table 3. Descriptive statistics of remotely sensed and modeled soil properties for the estimation of modified K-factor values.

Descriptive Statistics	AWC (%)	Psoil (mm/h)	BD (g/cm^3)	EVI	SR (%)	LAI (%)	A (%)	S (%)
Mean	0.39	58.18	1.04	0.33	0.85	1.55	0.286	3.54
Minimum	0.13	27.67	0.98	0.11	0.26	0.3	0.0013	0.74
Maximum	0.73	650	1.53	0.6	1	10	0.699	13.78

4. Discussions

4.1. Predictions of Kmlr Versus K_{USLE}

Figure 3a suggests that there was notable variation in soil erodibility factors across the different subbasins (1 through 7). In most subbasins, Kmlr values were generally lower

than K_{USLE} values, suggesting that modifications to the soil assessment approach may indicate less erodibility than traditionally measured by USLE factors. This could imply that the modified factors considered additional variables or improved methodologies that show the soil to be less prone to erosion. The presence of error bars indicates variability and uncertainty in the data for both Kmlr and K_{USLE} factors. Subbasin 4, for instance, exhibited a significant range in both Kmlr and K_{USLE} values, indicating potential complexities in soil behavior or assessment methods in that area. Subbasin 4 showed the highest average values for both Kmlr and K_{USLE}, highlighting it as a critical area potentially at higher risk for erosion when compared with other subbasins.

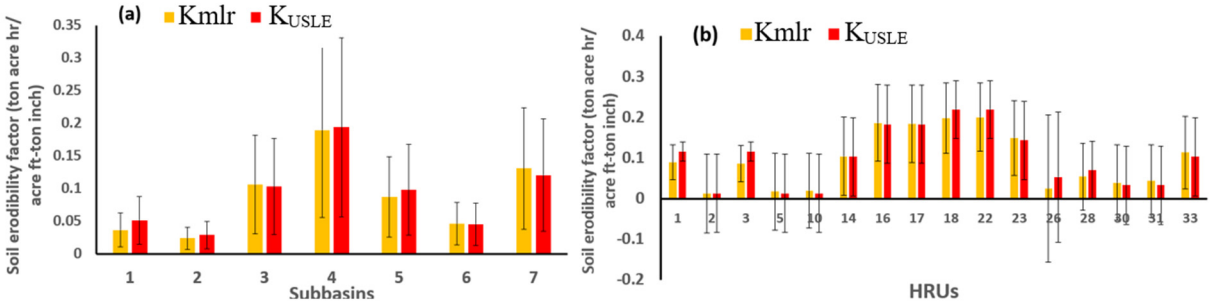


Figure 3. A comparison of the soil erodibility factors, Kmlr and K_{USLE} for the Fish River watershed. (**a**) Spatial extent of each subbasin (n = 7); (**b**) spatial extent of selected HRUs (n = 16).

The findings may suggest the need for tailored soil conservation practices in subbasins showing high erodibility. Understanding those areas that are more susceptible can help in prioritizing soil management and intervention strategies. For Figure 3, the large error could be due to the spatial or temporal scale of the analysis. In regions with complex landscapes as observed in the Fish River watershed, even slight changes in dynamic factors such as soil moisture or land cover can have significant effects on predictions. The K_{USLE} and Kmlr models have not yet fully captured this complexity, resulting in errors that appeared larger than expected.

Figure 3b reveals significant variability in soil erodibility factors across the different HRUs (1 to 33). In many HRUs, Kmlr values were either similar to or lower than K_{USLE} values, indicating that the modified method may reflect potentially lower erosion susceptibility under certain conditions. This difference suggests that the modified approach may have identified factors affecting soil stability that were not fully accounted for in the traditional USLE methodology. The errors accompanying both Kmlr and K_{USLE} measurements highlight the uncertainty and variability of the data. The HRUs (2 and 26) at the higher end of the scale displayed pronounced variability, suggesting a complex relationship impacting erodibility in those areas. HRUs 16, 18, and 28 exhibited some of the highest soil erodibility factors, indicating these might be critical areas for monitoring and management to mitigate erosion risks. Several HRUs showed Kmlr factors that fell below 0.1, particularly HRUs 1, 3, and 5, which suggests that these HRUs are relatively stable compared with others. The presence of HRUs with markedly high K_{USLE} values in relation to Kmlr underscores the importance of reassessing soil management practices, as the traditional methods might overstate the erosion risk for these areas. The results highlight the need for strategic soil conservation measures in HRUs with higher K_{USLE} values. The findings suggest that updated models such as Kmlr could be crucial for targeted interventions, potentially leading to more effective erosion control practices.

4.2. K_{USLE} and Kmlr Effects on Sediment Yield Predictions

Figure 4a indicates a positive relationship between the K_{USLE}-based sediment yield predictions, but the low R^2 value (0.08) suggests a weak correlation. This indicates that changes in the K_{USLE} resulted in only a small predictive ability regarding sediment yield within the subbasins of the watershed. The blue regression line shows a steeper slope compared with the traditional USLE approach, suggesting that sediment yield was more responsive to changes in the modified K-factor model, Kmlr (R^2 = 0.31). This indicates a moderately stronger relationship between the Kmlr and sediment yield distribution in the seven subbasins of the watershed. The Kmlr model. developed with the aid of pedotransfer functions considering the soil surface moisture and soil bulk density into the K-factor evaluation process, was more effective in predicting sediment yield in the studied areas than K_{USLE}. While both methods showed trends, the results imply that further investigation is needed to understand why the modified K-factor, Kmlr, estimates did not exhibit a much stronger correlation (close to 1) with sediment yield. This could lead to more refined models for predicting soil erosion and sediment transport in the landscape. For Figure 4, a weak correlation was observed, and the models used in the study showed fitting significances of $p < 0.01$. While the model may not explain all the variability in the data, it could still offer useful insights and serve as a foundation for further model refinement.

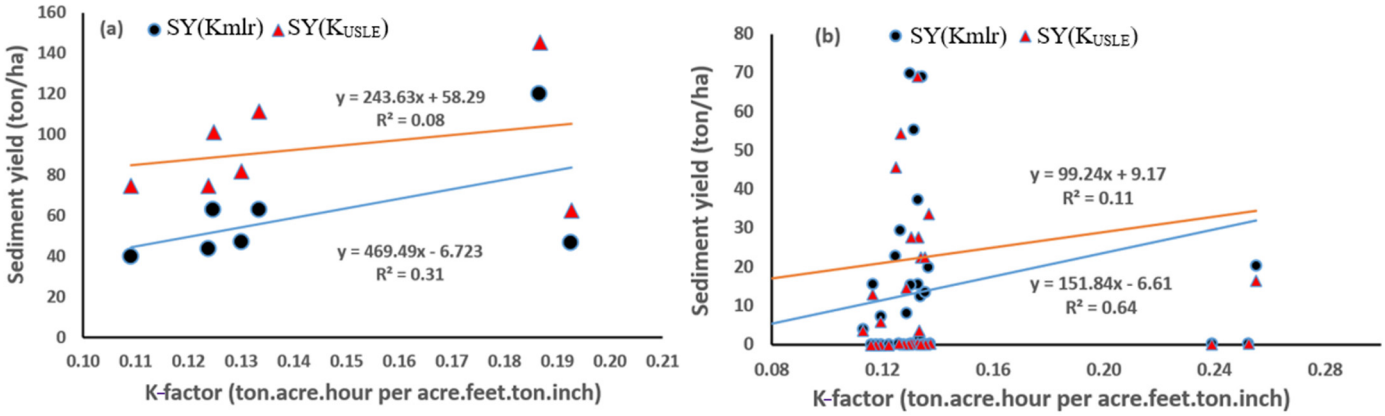


Figure 4. Effect of modification of K-factors (Kmlr compared with K_{USLE}) and corresponding shares of annual sediment yields averaged between 2001 and 2011 (**a**) for each subbasin (7 × 11) ($p < 0.01$) (**b**) for each HRU (36 × 11) ($p < 0.01$).

Figure 4b provides a comparison of sediment yields in relation to K-factor values, specifically focusing on Kmlr and K_{USLE}. The blue regression line corresponds to Kmlr. showing a R^2 value of 0.64 and suggesting a moderately strong correlation. It indicates that the modified K-factor, Kmlr, had a better predictive capacity for sediment yield when analyzed across HRUs than the traditional K_{USLE} method, which had a low R^2 value of 0.11. The results imply that Kmlr is a better model that explains a greater proportion of the variability in sediment yield than the traditional K_{USLE}. The results indicate that adaptations in the K-factor can lead to improved predictive capacity for sediment yield in HRUs, reinforcing the importance of selecting suitable models accounting for land cover change and soil structural and textural properties for estimating soil erosion. The findings point to the modified K-factor being more effective in predicting sediment yield within the studied HRUs relative to subbasins, which could be due to the lesser number and greater area of subbasins compared with HRUs in the watershed. This suggests potential advantages in using a tailored K-factor for better soil erosion management and sediment yield predictions in specific landscapes capturing improved spatial soil vulnerability as in

the case of HRUs. Further research could explore the reasons behind these variances and their applicability in different scenarios.

4.3. Spatial Effects of K-Factors on Sediment Yields

Figure 5a illustrates a comparative analysis of K-factors from various approaches for various modeling approaches, including K_{USLE}, Kmlr, Kmlr-sat, Kmlr-c, and Kmlr-dsat, across the seven subbasins of the Fish River watershed. The graph depicts varying K-factor values across the seven subbasins, highlighting that subbasin 5 exhibited the highest K-factor across all models. This elevated value suggests that this area is more susceptible to erosion, emphasizing the need for targeted management strategies. The results also suggest that K_{USLE} may underestimate the actual erosion potential in the watershed compared with the more dynamic approaches (Kmlr, Kmlr-sat, and Kmlr-c). Kmlr showed a significant increase in K-factor estimates, particularly in subbasin 5. Kmlr-sat, Kmlr-c, and Kmlr-dsat appeared to provide more refined estimates than K_{USLE} but still did not capture the extent of variability seen in the other approaches. Kmlr-dsat slightly overpredicted the K-factors (subbasins 2, 5, 6, 7) relative to the other two modified approaches of Kmlr-sat and Kmlr-c. This suggests that while the modified K-factor models incorporate some dynamic aspects, they may not fully leverage the capabilities of satellite data. There was a clear trend that the advanced models (Kmlr, Kmlr-dsat, Kmlr-c) yielded higher and more variable K-factor estimates, highlighting the importance of incorporating high-resolution soil surface moisture data and dynamic crop and cover management factors together, which could significantly enhance the estimation of soil erodibility across the Fish River watershed compared with traditional methods. In addition, the K-factor estimates for subbasin 5 underscore the necessity for localized assessment and potential conservation strategies to mitigate erosion risks.

The radar chart in Figure 5b illustrates the comparative correlations of sediment yields relative to different K-factor models across subbasins. The plotted lines suggest substantial variability in sediment yield correlations among the various models. Each subbasin appeared to display distinct performance patterns, indicating that soil erodibility and sediment transport behaviors differed spatially.

The modified K-factor model Kmlr-c generally showed higher correlation values across many subbasins, indicating that this method effectively estimated sediment yields as shown in Figure 5b. The Kmlr-sat correlations were more erratic, with values dropping significantly in some subbasins. This inconsistency suggests that the Kmlr-sat model may struggle to accurately predict sediment yields under varying conditions. Several models, particularly Kmlr-dsat and Kmlr-sat, exhibited negative correlations in certain subbasins. This indicates that these models may not align well with actual sediment yield behavior in those areas, suggesting potential misinterpretations in their soil-data integration. While K_{USLE} often scored high, Kmlr models demonstrated fluctuating performance, suggesting potential sensitivity to local conditions in specific subbasins. This underscores the importance of local calibration for soil erosion modeling. The variations highlight the need for careful selection and validation of erosion models based on subbasin characteristics. Selection of Kmlr-c may prove beneficial in accurate sediment yield assessments.

Figure 5c illustrates the correlations between sediment yields derived from the K-factor models. The K_{USLE} model showed a strong positive correlation with its SY. This indicates that the K_{USLE} was effective in estimating sediment yield based on the factors it accounted for. This could be attributed to the default K-factor and SY functionalities in the SWAT model algorithm, well calibrated inbuilt data inputs, and their direct discretization in the subbasin-wide simulations. The Kmlr model's correlation appeared to be moderate to high, suggesting that it effectively predicted sediment yield. The Kmlr-sat model showed

a negative correlation, meaning it may not accurately represent SY. The correlations of Kmlr-c and Kmlr-dsat were mixed, with Kmlr-c showing generally positive relationships. This variability points to different operational strengths and weaknesses of these models in dealing with sediment yield predictions. Understanding these correlations is essential for selecting the right model for predicting erosion and sediment yield in watershed management. It underscores the importance of model accuracy and adaptability to improve predictions in variable conditions.

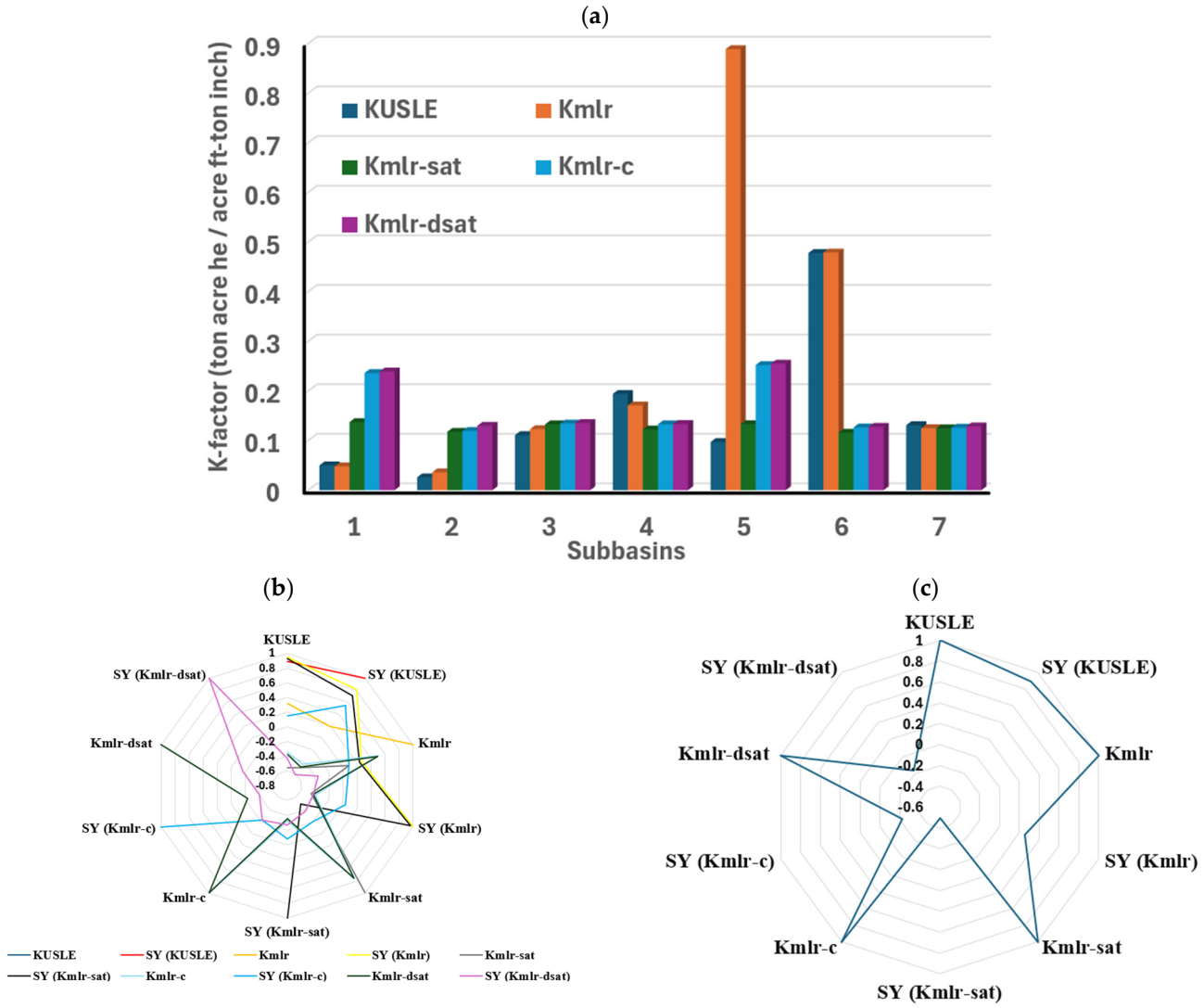


Figure 5. (**a**) A comparison of the soil erodibility factors developed from various approaches, K_{USLE}, Kmlr, Kmlr-sat, Kmlr-c, and Kmlr-dsat, (**b**) the corresponding sediment yield predictions, SY (K_{USLE}), SY (Kmlr), SY (Kmlr-sat), SY (Kmlr-c), and SY (Kmlr-dsat), averaged between 2001 and 2011 for the Fish River watershed for spatial extent of each subbasins (n = 7), and (**c**) correlations between sediment yields derived from the various K-factor models.

4.4. Validation of Sediment Yield Predictions: K_{USLE} vs. Kmlr-c

From the results of the descriptive statistics and spatial analysis of traditional and novel approaches of K-factors and the resulting SY estimates, the K_{USLE}, Kmlr, Kmlr-c, and Kmlr-dsat models were found to showcase notable relationship trends. Hence, the simulated SY based on these models, K_{USLE}, Kmlr, Kmlr-c, and Kmlr-dsat, were validated against observed SY. Figure 6a illustrates the relationship between observed and simulated sediment yield values for the two best performing K-factor models for the Lower Fish River watershed at Silver Hill station. The blue line represents the regression line for

the SY predictions based on Kmlr-c against observed SY, with an R^2 value of 0.980. This strong R^2 indicates a very close fit between the simulated values and the observed data, suggesting that the modified approach accurately predicted sediment yield. The orange line shows the regression line for the SY predictions based on the traditional USLE method, K_{USLE}, with an R^2 value of 0.911. This also indicates a strong correlation, but with a slope less than 1, suggesting the USLE underestimated sediment yield compared with the observed data. Both models demonstrated strong relationships with observed sediment yield, though the modified K-factor with a union of dynamic C-factor estimates and high-resolution satellite data on AWC, SR, LAI, and EVI slightly overestimated yields concerning observed values, while the USLE underestimated. The closeness of the SYobs and SY(Kmlr-c) indicates that Kmlr-c may be better calibrated for these specific conditions of the watershed and thus provides a more accurate representation of sediment dynamics. The results underscore the effectiveness of modifying existing models (such as USLE) with the additional enhancements of a completely remotely sensed data-based function of crop and cover management factor and high-resolution soil moisture data to enhance predictions based on localized conditions, which is crucial for effective soil erosion management and watershed management strategies.

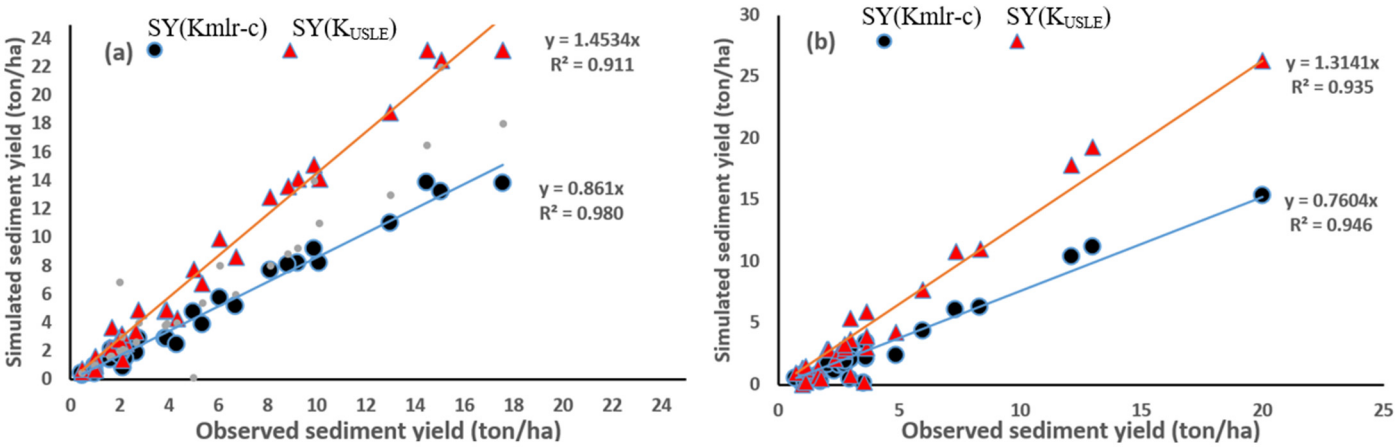


Figure 6. Scatter plot for the years between 2001 and 2011 for observed, USLE-based, and modified monthly values of sediment yield (SYobs, SY (K_{USLE}), and SY (Kmlr-c), respectively) for (**a**) the Lower Fish River watershed at Silver Hill station (n = 32) and (**b**) the Middle Fish River watershed at Loxley station (n = 34).

Figure 6b indicates a strong relationship between the modified model's simulated sediment yield, SY(Kmlr-c), and the observed sediment yield, SYobs, suggesting that the modified approach captured sediment dynamics very effectively (R^2 value of 0.946). The slope of less than 1 indicates that the modified model slightly underestimated the observed sediment yield at higher values at the Middle Fish River watershed at Loxley station. The strong R^2 of 0.935 between SYobs and SY (K_{USLE}) indicates that the USLE also captured sediment yield accurately; however, the slope being greater than 1 suggests that the system tended to overestimate sediment yield at higher observed values compared with what was actually observed. The results pinpoint that both models indicated strong predictive relationships with observed sediment yield, as supported by high R^2 values. However, the SY based off of the modified K-factor model, SY (Kmlr-c), appeared to provide a more consistent underestimation at higher observed yields, which might be beneficial for conservation practices where overestimating yield could lead to mismanagement. The USLE model sometimes overestimated yield, particularly at larger values, which may suggest parameters in the USLE configuration require adjustment for this watershed. The findings indicate both simulation methods were robust for estimating sediment yield

in the Middle Fish River watershed, with the modified K-factor demonstrating slightly improved performance in some ranges of observed sediment yield. These insights support the idea that refining existing models using high-resolution satellite data and modification of dependent variables in the K-factor model (Cdynamic development and inclusion into the Kmlr model to form Kmlr-c) can enhance predictive capabilities, leading to better management strategies for soil erosion and sediment control. Overall, the study results highlight that the Kmlr-c model, which integrates high-resolution satellite data for factors such as soil surface moisture, solar radiation, leaf area index, and enhanced vegetation index, provides a more accurate representation of sediment dynamics and is thus a better predictor of SY. Future investigations could focus on optimizing both models further or investigating additional factors influencing sediment yield in this and other watersheds.

4.5. Sediment Yield Predictions and Soil Loss Representation

Table 4 provides a statistical summary of the K-factors (erosion susceptibility), sediment yields (SY (K_{USLE}) and SY (Kmlr-c)), and differences in soil loss across 36 HRUs in various subbasins. The area for each HRU varied widely, from small areas of 612.35 ha to larger areas of up to 5924.73 ha, which influenced the overall sediment yield and soil loss.

The dominant land uses included wetland, agriculture, hay, forest, and urban development. The difference between the modified sediment yield and the USLE-based sediment yield is indicative of the soil loss representation based on K-factor prediction approaches. The range of K-factors varied across the HRUs, from 0.0572 (wetland, subbasin 7, HRU 36) to 0.2550 (agriculture, subbasin 5, HRU 26), reflecting the vulnerability of soils in different land uses to erosion. Wetlands generally showed low K-factors and relatively low sediment yields. HRUs such as 36 and 3 had low K-factors (0.0572 and 0.2362) and moderate differences in soil loss, suggesting that wetlands help reduce soil erosion and sediment loss. Agricultural areas tended to have higher K-factors, leading to higher sediment yields. HRU 34 in subbasin 7 (agriculture) had a K-factor of 0.1286 and a soil loss difference of 6.552 ton/ha, showing substantial soil loss. Forests typically had lower K-factors and lower sediment yields, indicating that forest cover helps prevent erosion. HRUs such as 28 and 12 with forest land use had low K-factors and negligible differences in soil loss. In some HRUs, the modified sediment yield was higher than the USLE-based sediment yield, suggesting that the modified model considered factors that led to a prediction of more soil erosion than the USLE model. HRU 35 in subbasin 7 showed a large, positive difference (22.889 ton/ha), indicating significant soil loss in this area when the modified model was used.

Some HRUs, particularly those in agricultural areas, showed negative differences, suggesting that the modified model predicted less soil loss than the USLE model. HRU 24 in subbasin 5 (agriculture) showed a difference of −0.062 ton/ha; the modified model predicted slightly less soil erosion than the USLE. Several HRUs, particularly those in wetland areas such as HRU 10 (subbasin 2) and HRU 36 (subbasin 7), showed very high modified sediment yields (69.776 ton/ha and 103.865 ton/ha), leading to substantial soil loss differences when compared with the USLE. These areas may be facing severe erosion due to land use changes or inadequate soil conservation practices. HRUs with low soil loss include those under forest cover, such as HRUs 28 and 12, where soil loss was minimal, highlighting the effectiveness of forested land in preventing erosion. The findings suggest that specific land uses such as wetlands and forests offer protection against erosion, while agricultural areas tend to be more susceptible to significant soil loss. The use of modified models could improve soil loss predictions, particularly in areas where land use and other environmental factors contribute to higher erosion than estimated by USLE. In the watershed level, the USLE method (828.624 ton/ha) overpredicted the sediment yield relative to the modified K-factor method (525.112 ton/ha).

Table 4. Statistical summary of the modified K-factors, comparison of modified sediment yields against USLE based sediment yields, and the differences in soil loss for 36 HRUs.

Subbasin Number	HRU Number	HRU Area (ha)	Landuse	Kmlr-c	SY (Kmlr-c) (ton/ha)	SY (K_{USLE}) (ton/ha)	Difference in Soil Loss
7	36	1366.19	Wetland	0.0572	1.337	2.229	0.892
6	32	1536.97	Wetland	0.113	3.936	3.578	−0.357
6	28	1271.14	Forest	0.1159	0.005	0.004	−0.001
2	11	1676.87	Wetland	0.1165	15.595	12.994	−2.6
2	8	3686.9	Hay	0.1177	0.016	0.014	−0.003
4	22	712.35	Wetland	0.1193	7.176	5.979	−1.196
2	6	2695.56	Forest	0.1194	0.006	0.005	−0.001
4	18	819.7	Forest	0.1222	0.006	0.005	−0.001
7	35	1366.19	Wetland	0.1247	22.861	45.75	22.889
7	33	829.77	Hay	0.1259	0.136	0.251	0.115
6	31	1536.97	Wetland	0.1264	29.397	54.344	24.947
6	29	2724.73	Hay	0.1276	0.104	0.194	0.09
7	34	2609.36	Agriculture	0.1286	8.099	14.652	6.552
6	27	1271.14	Forest	0.1293	0.099	0.183	0.084
2	10	1676.87	Wetland	0.1299	69.776	129.004	59.228
5	23	2477.26	Hay	0.1302	0.231	0.428	0.196
6	30	2283.32	Agriculture	0.1303	15.366	27.576	12.21
2	7	3686.9	Hay	0.1311	0.17	0.313	0.144
3	15	914.17	Wetland	0.1314	55.264	102.171	46.907
3	13	2464.32	Hay	0.1326	0.163	0.302	0.139
4	21	712.35	Wetland	0.1327	37.321	68.995	31.674
2	5	2695.56	Forest	0.1328	0.188	0.348	0.16
5	25	3525.72	Agriculture	0.1329	15.645	27.566	11.921
4	16	613.8	Urban	0.1334	1.962	3.604	1.642
2	9	4170.06	Agriculture	0.1338	12.548	22.531	9.983
4	19	1295.96	Hay	0.1339	0.119	0.22	0.101
1	4	2040.65	Wetland	0.1343	69.024	127.612	58.588
3	12	1261.68	Forest	0.1343	0.174	0.32	0.146
3	14	2933.56	Agriculture	0.1353	13.477	22.456	8.978
4	17	819.7	Forest	0.1356	0.105	0.181	0.076
4	20	711.38	Agriculture	0.1366	19.935	33.742	13.807
1	2	5924.73	Forest	0.1372	0.181	0.31	0.129
1	3	2040.65	Wetland	0.2362	103.865	103.865	0
1	1	5924.73	Forest	0.2391	0.201	0.201	0
5	24	2477.26	Hay	0.2523	0.309	0.247	−0.062
5	26	3525.72	Agriculture	0.255	20.315	16.45	−3.865
Total					525.112	828.624	303.512

4.6. Categorization of Erosive Hotspots

Table 5 details the categorization of erosive hotspots based on the best performing K-factor model (Kmlr-c) outcomes. Erosive hotspot identification revealed that 6003 ha of land (7.7% of the watershed) was at high erosion risk (K > 0.25), with an average soil loss of 24.2 ton/ha. On the other hand, 63,000+ ha was classified as low risk, demonstrating the ability of the modified model to accurately categorize erosion-prone regions. The results point out that the improved model also accounted for spatial variations in soil properties, particularly in agricultural and wetland regions, where USLE-based methods failed to capture dynamic soil moisture influences. The K-factor category of Very Low indicates areas that have minimal erosion risk, likely due to stable land use, low slopes, or protective vegetation cover. Although the land area in this category was relatively small (1366.19 ha), soil loss remained very low, with only 0.20 tons of soil lost per hectare. Most of the land in the watershed (62,945.64 ha) fell under the Low category of K-factor, suggesting that a significant portion of the area has low erosion potential. Despite the larger area, the soil loss was moderate (492.48 ton/ha), indicating that these areas may have moderate slopes, some vulnerability to erosion, or land use that does not fully protect the soil but still prevents severe erosion. The regions with K-factors ranging from 0.15 to 0.25 (Medium) were more vulnerable to soil loss than the previous categories, with a soil loss of 8.24 ton/ha. While the total area was relatively small (7965.38 ha), these areas were likely to experience higher erosion due to steeper slopes, less protective vegetation, or land use practices that exacerbate soil erosion. The K-factor category High identifies areas at high risk for soil erosion, with the K-factor indicating severe erosion potential (0.25–0.30). Although the total land area was small (6002.99 ha), the soil loss in these areas was significant (24.20 ton/ha). These areas likely have steep slopes and/or poor land management practices, leading to higher levels of erosion. The total area across all categories was 78,280.20 ha, with a combined soil loss of 525.11 ton/ha. Most of the land was categorized as "Low" erosion risk, with relatively low soil loss per hectare, indicating that most of the watershed is protected against severe erosion. However, the high and medium erosion categories, though smaller in area, suggest that there are critical areas that need attention in terms of erosion control, land management, and potentially soil conservation measures.

Table 5. Categorization of soil erosion hotspots, area ratios of HRUs, and the amount of soil loss for the Fish River watershed based on the modified K-factor model, Kmlr-c.

Erosion Categories	Kmlr-c range (ton . acre hour per acre feet ton inch)	Area Land Use (ha)	Area Soil (ha)	Area Slope (ha)	Soil Loss (ton/ha)
Very Low	0.00–0.05	1366.19	279.1	279.1	0.2
Low	0.05–0.15	62,945.64	42,523.68	42,523.68	492.48
Medium	0.15–0.25	7965.38	5655.56	5655.56	8.24
High	0.25–0.30	6002.99	2087.8	2087.8	24.2
Total		78,280.2	50,546.15	50,546.15	525.11

5. Conclusions

Soil erosion remains a critical challenge for soil health and agricultural productivity, with the K-factor commonly used to assess soil erodibility in models such as the Universal Soil Loss Equation. However, traditional methods often lack spatiotemporal accuracy, particularly when accounting for dynamic factors such as soil moisture and land cover variations. This study presents a modified K-factor pedotransfer function (Kmlr) that integrates dynamic, remotely sensed data on land use land cover, to improve the accuracy

of K-factor estimates for diverse soil health management applications. The Kmlr model, incorporating high-resolution MODIS-based soil surface moisture (Kmlr-sat), dynamic crop and cover management factors, Cdynamic (Kmlr-c), and downscaled soil surface moisture data from SMAP (Kmlr-dsat), was tested across spatial and temporal scales within the Fish River watershed in Alabama, a coastal region with complex soil–water interactions.

Results show that the Kmlr model, augmented by dynamic soil moisture and land cover data, significantly enhanced spatial accuracy in estimating soil erodibility. The Kmlr K-factor values were generally lower than those of the USLE, suggesting that the modified approach reflected less erodibility in certain areas, likely because of to additional dynamic factors considered in the model. Traditional USLE-based models overestimated sediment yield by up to 59.23 ton/ha in high-risk areas, while the total predicted sediment yield in the watershed was 828.62 ton/ha for USLE-based estimates, compared with 525.11 ton/ha using Kmlr-c. Sediment yield predictions using the modified Kmlr-c model demonstrated the strongest correlation with observed sediment yield (R^2 = 0.980), outperforming the USLE model (R^2 = 0.911). This suggests that the modified Kmlr-c model, which integrates high-resolution satellite data for factors such as soil surface moisture, solar radiation, leaf area index, and enhanced vegetation index, provides a more accurate representation of sediment dynamics. While both models showed strong relationships with observed sediment yield, the modified Kmlr-c model had slightly better calibration for the specific landscape conditions of the watershed, offering more accurate predictions. The analysis of sediment yield across 36 HRUs further highlighted the advantages of the modified Kmlr model in predicting soil loss. Areas with high land use variations, such as wetlands, agriculture, and forested regions, exhibited significant differences in soil loss between the modified and USLE-based models. These findings underscore the need for more tailored soil conservation strategies in regions with high erosion risk.

The categorization of erosive hotspots in the watershed reveals that most areas fell under the "Low" K-factor category, with moderate soil loss. However, critical areas identified as "High" or "Medium" risk, although smaller in size, represented regions that require immediate attention for erosion control and land management interventions. Erosive hotspot identification revealed that 6003 ha of land (7.7% of the watershed) was at high erosion risk (K > 0.25), with an average soil loss of 24.2 ton/ha. Conversely, 63,000+ ha was classified as low-risk areas, demonstrating the ability of the modified model to accurately categorize erosion-prone regions. The improved model also accounted for spatial variations in soil properties, particularly in agricultural and wetland regions, where USLE-based methods failed to capture dynamic soil moisture influences. The results demonstrate the potential of the modified K-factor model to enhance soil erosion predictions, guiding more effective watershed management strategies. This research highlights the importance of refining traditional K-factor models using dynamic, remotely sensed data and tailored approaches such as Kmlr-c. The study outcomes signify that with a union of dynamic crop and cover management estimates and high-resolution satellite data on soil surface moisture, sediment yield and soil loss predictions could be improved, thus enhancing soil health assessments and contributing to better management practices for soil conservation and ecosystem resilience.

Author Contributions: Conceptualization, methodology, data curation, and writing—P.P.; conceptualization, review, and editing—N.J. All authors have read and agreed to the published version of the manuscript.

Funding: This work was partially funded by the NSF grant OIA 2019561.

Data Availability Statement: Data will be available upon request.

Acknowledgments: I would like to acknowledge the reviewers for enhancing the article.

Conflicts of Interest: The authors declare no conflict of interest.

References

1. Montgomery, D.R. Soil erosion and agricultural sustainability. *Proc. Natl. Acad. Sci. USA* **2007**, *104*, 13268–13272. [CrossRef] [PubMed]
2. Pierce, F.J.; Lal, R. Monitoring the impact of soil erosion on crop productivity. In *Soil Erosion Research Methods*; Routledge: London, UK, 2017; pp. 235–263.
3. Akhtar, N.; Syakir Ishak, M.I.; Bhawani, S.A.; Umar, K. Various natural and anthropogenic factors responsible for water quality degradation: A review. *Water* **2021**, *13*, 2660. [CrossRef]
4. Preetha, P.P.; Johns, M. A review of recent water quality assessments in watersheds of southeastern United States using continuous time models. *Glob. J. Eng. Sci.* **2022**, *9*, 1–4. [CrossRef]
5. Steinhoff-Knopp, B.; Kuhn, T.K.; Burkhard, B. The impact of soil erosion on soil-related ecosystem services: Development and testing a scenario-based assessment approach. *Environ. Monit. Assess.* **2021**, *193* (Suppl. S1), 274. [CrossRef] [PubMed]
6. Wischmeier, W.H. *Predicting Rainfall-Erosion Losses from Cropland East of the Rocky Mountains, Guide for Selection of Practices for Soil and Water Conservation*; United States Government Printing Office: Washington, DC, USA, 1965.
7. Römkens, M.J.M.; Young, R.A.; Poesen, J.W.A.; McCool, D.K.; El-Swaify, S.A.; Bradford, J.M. Soil erodibility factor (K). In *Predicting Soil Erosion by Water: A Guide to Conservation Planning with the Revised Universal Soil Loss Equation (RUSLE)*; Renard, K.G., Foster, G.R., Weesies, G.A., McCool, D.K., Yoder, D.C., Eds.; Agric. HB: Washington, DC, USA, 1997; pp. 65–99.
8. Alewell, C.; Borrelli, P.; Meusburger, K.; Panagos, P. Using the USLE: Chances, challenges and limitations of soil erosion modelling. *Int. Soil Water Conserv. Res.* **2019**, *7*, 203–225. [CrossRef]
9. Auerswald, K.; Fiener, P.; Martin, W.; Elhaus, D. Use and misuse of the K factor equation in soil erosion modeling: An alternative equation for determining USLE nomograph soil erodibility values. *Catena* **2014**, *118*, 220–225. [CrossRef]
10. Merritt, W.S.; Letcher, R.A.; Jakeman, A.J. A review of erosion and sediment transport models. *Environ. Model. Softw.* **2003**, *18*, 761–799. [CrossRef]
11. Lin, B.S.; Chen, C.K.; Thomas, K.; Hsu, C.K.; Ho, H.C. Improvement of the K-factor of USLE and soil erosion estimation in Shihmen reservoir watershed. *Sustainability* **2019**, *11*, 355. [CrossRef]
12. Lal, R.A.T.T.A.N. Soil degradation by erosion. *Land Degrad. Dev.* **2001**, *12*, 519–539. [CrossRef]
13. Rajbanshi, J.; Bhattacharya, S. Assessment of soil erosion, sediment yield and basin specific controlling factors using RUSLE-SDR and PLSR approach in Konar river basin, India. *J. Hydrol.* **2020**, *587*, 124935. [CrossRef]
14. Andualem, T.G.; Hewa, G.A.; Myers, B.R.; Peters, S.; Boland, J. Erosion and sediment transport modeling: A systematic review. *Land* **2023**, *12*, 1396. [CrossRef]
15. Renard, K.G.; Ferreira, V.A. RUSLE model description and database sensitivity. *J. Environ. Qual.* **1993**, *22*, 458–466. [CrossRef]
16. Preetha, P.P.; Joseph, N.; Narasimhan, B. Quantifying surface water and ground water interactions using a coupled SWAT_FEM model: Implications of management practices on hydrological processes in irrigated river basins. *Water Resour. Manag.* **2021**, *35*, 2781–2797. [CrossRef]
17. Gonzalez, M.O.; Preetha, P.; Kumar, M.; Clement, T.P. Comparison of data-driven groundwater recharge estimates with a process-based model for a river basin in the southeastern USA. *J. Hydrol. Eng.* **2023**, *28*, 04023019. [CrossRef]
18. Preetha, P.P.; Maclin, K. Evaluation of Hydrogeological Models and Big Data for Quantifying Groundwater Use in Regional River Systems. In *Environmental Processes and Management: Tools and Practices for Groundwater*; Springer International Publishing: Cham, Switzerland, 2023; pp. 189–206.
19. Admas, M.; Melesse, A.M.; Abate, B.; Tegegne, G. Soil erosion, sediment yield, and runoff modeling of the megech watershed using the GeoWEPP model. *Hydrology* **2022**, *9*, 208. [CrossRef]
20. Worku, Y.A.; Moges, A.; Kendie, H. Comparison of SWAT and WEPP for Modeling Annual Runoff and Sediment Yield in Agewu-Mariyam Watershed, Northern Ethiopia. *Int. J. Food Agric. Nat. Resour.* **2024**, *5*, 104–113. [CrossRef]
21. Meshram, S.G.; Singh, V.P.; Kisi, O.; Karimi, V.; Meshram, C. Application of artificial neural networks, support vector machine and multiple model-ANN to sediment yield prediction. *Water Resour. Manag.* **2020**, *34*, 4561–4575. [CrossRef]
22. Essam, Y.; Huang, Y.F.; Birima, A.H.; Ahmed, A.N.; El-Shafie, A. Predicting suspended sediment load in Peninsular Malaysia using support vector machine and deep learning algorithms. *Sci. Rep.* **2022**, *12*, 302. [CrossRef]
23. Hu, J.; Miao, C.; Zhang, X.; Kong, D. Retrieval of suspended sediment concentrations using remote sensing and machine learning methods: A case study of the lower Yellow River. *J. Hydrol.* **2023**, *627*, 130369. [CrossRef]
24. Paulista, R.S.D.; de Almeida, F.T.; de Souza, A.P.; Hoshide, A.K.; de Abreu, D.C.; da Silva Araujo, J.W.; Martim, C.C. Estimating Suspended Sediment Concentration using Remote Sensing for the Teles Pires River, Brazil. *Sustainability* **2023**, *15*, 7049. [CrossRef]
25. Qi, L.; Zhou, Y.; Van Oost, K.; Ma, J.; van Wesemael, B.; Shi, P. High-resolution soil erosion mapping in croplands via Sentinel-2 bare soil imaging and a two-step classification approach. *Geoderma* **2024**, *446*, 116905. [CrossRef]

26. Sotiri, K.; Hilgert, S.; Duraes, M.; Armindo, R.A.; Wolf, N.; Scheer, M.B.; Kishi, R.; Pakzad, K.; Fuchs, S. To what extent can a sediment yield model be trusted? A case study from the Passauna Catchment, Brazil. *Water* **2021**, *13*, 1045. [CrossRef]
27. Benavidez, R.; Jackson, B.; Maxwell, D.; Norton, K. A review of the (Revised) Universal Soil Loss Equation ((R) USLE): With a view to increasing its global applicability and improving soil loss estimates. *Hydrol. Earth Syst. Sci.* **2018**, *22*, 6059–6086. [CrossRef]
28. Swarnkar, S.; Tripathi, S.; Sinha, R. Understanding hydrogeomorphic and climatic controls on soil erosion and sediment dynamics in large Himalayan basins. *Sci. Total Environ.* **2021**, *795*, 148972. [CrossRef] [PubMed]
29. Preetha, P.; Al-Hamdan, A. A union of dynamic hydrological modeling and satellite remotely-sensed data for spatiotemporal assessment of sediment yields. *Remote Sens.* **2022**, *14*, 400. [CrossRef]
30. Qi, J.; Li, S.; Yang, Q.; Xing, Z.; Meng, F.R. SWAT setup with long-term detailed landuse and management records and modification for a micro-watershed influenced by freeze-thaw cycles. *Water Resour. Manag.* **2017**, *31*, 3953–3974. [CrossRef]
31. Wang, J.; Yang, J.; Li, Z.; Ke, L.; Li, Q.; Fan, J.; Wang, X. Research on Soil Erosion Based on Remote Sensing Technology: A Review. *Agriculture* **2024**, *15*, 18. [CrossRef]
32. Abdulraheem, M.I.; Zhang, W.; Li, S.; Moshayedi, A.J.; Farooque, A.A.; Hu, J. Advancement of remote sensing for soil measurements and applications: A comprehensive review. *Sustainability* **2023**, *15*, 15444. [CrossRef]
33. Prasannakumar, V.; Shiny, R.; Geetha, N.; Vijith, H.J.E.E.S. Spatial prediction of soil erosion risk by remote sensing, GIS and RUSLE approach: A case study of Siruvani river watershed in Attapady valley, Kerala, India. *Environ. Earth Sci.* **2011**, *64*, 965–972. [CrossRef]
34. Ayalew, D.A.; Deumlich, D.; Šarapatka, B.; Doktor, D. Quantifying the sensitivity of NDVI-based C factor estimation and potential soil erosion prediction using Spaceborne earth observation data. *Remote Sens.* **2020**, *12*, 1136. [CrossRef]
35. Zhao, C.; Shao, M.A.; Jia, X.; Nasir, M.; Zhang, C. Using pedotransfer functions to estimate soil hydraulic conductivity in the Loess Plateau of China. *Catena* **2016**, *143*, 1–6. [CrossRef]
36. Ramos, T.B.; Darouich, H.; Gonçalves, M.C. Development and functional evaluation of pedotransfer functions for estimating soil hydraulic properties in Portuguese soils: Implications for soil water dynamics. *Geoderma Reg.* **2023**, *35*, e00717. [CrossRef]
37. Li, X.; Wang, H.; Qin, S.; Lin, L.; Wang, X.; Cornelis, W. Evaluating ensemble learning in developing pedotransfer functions to predict soil hydraulic properties. *J. Hydrol.* **2024**, *640*, 131658. [CrossRef]
38. Wang, W.; Huang, D.; Wang, X.G.; Liu, Y.R.; Zhou, F. Estimation of soil moisture using trapezoidal relationship between remotely sensed land surface temperature and vegetation index. *Hydrol. Earth Syst. Sci.* **2011**, *15*, 1699–1712. [CrossRef]
39. Silvero, N.E.Q.; Demattê, J.A.M.; Amorim, M.T.A.; dos Santos, N.V.; Rizzo, R.; Safanelli, J.L.; Poppiel, R.R.; de Sousa Mendes, W.; Bonfatti, B.R. Soil variability and quantification based on Sentinel-2 and Landsat-8 bare soil images: A comparison. *Remote Sens. Environ.* **2021**, *252*, 112117. [CrossRef]
40. da Silva, V.S.; Salami, G.; da Silva, M.I.O.; Silva, E.A.; Monteiro Junior, J.J.; Alba, E. Methodological evaluation of vegetation indexes in land use and land cover (LULC) classification. *Geol. Ecol. Landsc.* **2020**, *4*, 159–169. [CrossRef]
41. Jackson, T.J.; Bindlish, R.; Cosh, M.H.; Zhao, T.; Starks, P.J.; Bosch, D.D.; Seyfried, M.; Moran, M.S.; Goodrich, D.C.; Kerr, Y.H.; et al. Validation of Soil Moisture and Ocean Salinity (SMOS) soil moisture over watershed networks in the US. *IEEE Trans. Geosci. Remote Sens.* **2011**, *50*, 1530–1543. [CrossRef]
42. Kolli, M.K.; Opp, C.; Groll, M. Estimation of soil erosion and sediment yield concentration across the Kolleru Lake catchment using GIS. *Environ. Earth Sci.* **2021**, *80*, 161. [CrossRef]
43. Yadav, A.; Alam, M.A.; Suryavanshi, S. Daily sediment yield prediction using hybrid machine learning approach. *Int. J. Environ. Clim. Change* **2023**, *13*, 143–157. [CrossRef]
44. Arnold, J.G.; Moriasi, D.N.; Gassman, P.W.; Abbaspour, K.C.; White, M.J.; Srinivasan, R.; Santhi, C.; Harmel, R.D.; Van Griensven, A.; Van Liew, M.W.; et al. SWAT: Model use, calibration, and validation. *Trans. ASABE* **2012**, *55*, 1491–1508. [CrossRef]
45. Foster, G.R.; Lane, L.J.; Nowlin, J.D.; Laflen, J.M.; Young, R.A. Estimating erosion and sediment yield on field-sized areas. *Trans. ASAE* **1981**, *24*, 1253–1262. [CrossRef]
46. Flacke, W.; Auerswald, K.; Neufang, L. Combining a modified Universal Soil Loss Equation with a digital terrain model for computing high resolution maps of soil loss resulting from rain wash. *Catena* **1990**, *17*, 383–397. [CrossRef]
47. Williams, J.R. Sediment-yield prediction with universal equation using runoff energy factor. In *Present and Prospective Technology for Predicting Sediment Yield and Sources, Proceedings of the Sediment-Yield Workshop, USDA Sedimentation Laboratory, Oxford, MS, USA, 28–30 November 1972*; Agricultural Research Service, US Department of Agriculture: Stoneville, MS, USA, 1975; Volume 40, p. 244.
48. Kinnell, P.I.A.; Risse, L.M. USLE-M: Empirical modeling rainfall erosion through runoff and sediment concentration. *Soil Sci. Soc. Am. J.* **1998**, *62*, 1667–1672. [CrossRef]
49. Neitsch, S.L.; Arnold, J.G.; Kiniry, J.R.; Williams, J.R. *Soil and Water Assessment Tool Theoretical Documentation Version 2009*; Texas Water Resources Institute: College Station, TX, USA, 2011.
50. Preetha, P.P.; Al-Hamdan, A.Z. Multi-level pedotransfer modification functions of the USLE-K factor for annual soil erodibility estimation of mixed landscapes. *Model. Earth Syst. Environ.* **2019**, *5*, 767–779. [CrossRef]

51. Preetha, P.; Hasan, M. Scrutinizing the Hydrological Responses of Chennai, India Using Coupled SWAT-FEM Model under Land Use Land Cover and Climate Change Scenarios. *Land* **2023**, *12*, 938. [CrossRef]
52. Preetha, P.P.; Al-Hamdan, A.Z.; Anderson, M.D. Assessment of climate variability and short-term land use land cover change effects on water quality of Cahaba River Basin. *Int. J. Hydrol. Sci. Technol.* **2021**, *11*, 54–75. [CrossRef]
53. Mednick, A.C. Does soil data resolution matter? State Soil Geographic database versus Soil Survey Geographic database in rainfall-runoff modeling across Wisconsin. *J. Soil Water Conserv.* **2010**, *65*, 190–199. [CrossRef]
54. Preetha, P.P.; Al-Hamdan, A.Z. Synergy of remotely sensed data in spatiotemporal dynamic modeling of the crop and cover management factor. *Pedosphere* **2022**, *32*, 381–392. [CrossRef]
55. Zhang, R.; Kim, S.; Sharma, A. A comprehensive validation of the SMAP Enhanced Level-3 Soil Moisture product using ground measurements over varied climates and landscapes. *Remote Sens. Environ.* **2019**, *223*, 82–94. [CrossRef]
56. Preetha, P.P.; Al-Hamdan, A.Z. Developing nitrate-nitrogen transport models using remotely-sensed geospatial data of soil moisture profiles and wet depositions. *J. Environ. Sci. Health A* **2020**, *55*, 615–628. [CrossRef]
57. Preetha, P.P.; Al-Hamdan, A.Z. Integrating finite-element-model and remote-sensing data into SWAT to estimate transit times of nitrate in groundwater. *Hydrogeol. J.* **2020**, *28*, 2187–2205. [CrossRef]
58. Preetha, P.P.; Shirani-Bidabadi, N.; Al-Hamdan, A.Z.; Anderson, M. A methodical assessment of floodplains in mixed land covers encompassing bridges in Alabama state: Implications of spatial land cover characteristics on flood vulnerability. *Water Resour. Manag.* **2021**, *35*, 1603–1618. [CrossRef]

Disclaimer/Publisher's Note: The statements, opinions and data contained in all publications are solely those of the individual author(s) and contributor(s) and not of MDPI and/or the editor(s). MDPI and/or the editor(s) disclaim responsibility for any injury to people or property resulting from any ideas, methods, instructions or products referred to in the content.